Supplemental Document

Biomedical Optics EXPRESS

Spectral focusing-based stimulated Raman scattering microscopy using compact glass blocks for adjustable dispersion: supplement

Justin R. Gagnon,[1,†] Christian Harry Allen,[1,†] Dominique Trudel,[2,3,4] Frederic Leblond,[2,3,5] Peter K. Stys,[6] Craig Brideau,[6] and Sangeeta Murugkar[1,*]

[1]*Department of Physics, Carleton University, 1125 Colonel By Drive, Ottawa, Ontario, K1S 5B6, Canada*
[2]*Centre de recherche du Centre hospitalier de l'Université de Montréal, Montreal, Quebec, Canada*
[3]*Institut du cancer de Montréal, Montreal, Quebec, Canada*
[4]*Department of Pathology and cellular Biology, Université de Montréal 2900, boulevard Édouard-Montpetit, Montreal, Quebec, Canada*
[5]*Department of Engineering Physics, Polytechnique Montréal, 2500 chemin de Polytechnique, Montreal, Quebec, Canada*
[6]*Department of Clinical Neurosciences, University of Calgary, 3330 Hospital Drive N.W. HRIC 1B37A, Calgary, Alberta, T2N 4N1, Canada*
[†]*Contributed equally to this work.*
[*]*smurugkar@physics.carleton.ca*

Supplement DOI: https://doi.org/10.6084/m9.figshare.22633246

Parent Article DOI: https://doi.org/10.1364/BOE.486753

Supplementary Information: Spectral focusing-based stimulated Raman scattering microscopy using compact glass blocks for adjustable dispersion

JUSTIN R. GAGNON[1,†], CHRISTIAN HARRY ALLEN[1,†], DOMINIQUE TRUDEL[2,3,4], FREDERIC LEBLOND[2,3,5], PETER K. STYS[6], CRAIG BRIDEAU[6], AND SANGEETA MURUGKAR[1,*]

[1]Department of Physics, Carleton University, 1125 Colonel By Drive, Ottawa, Ontario, K1S 5B6, Canada
[2]Centre de recherche du Centre hospitalier de l'Université de Montréal, Montreal, Quebec, Canada
3Institut du cancer de Montréal, Montreal, Quebec, Canada
[4]Department of Pathology and cellular Biology, Université de Montréal 2900, boulevard Édouard-Montpetit, Montreal, Quebec, Canada
5Department of Engineering Physics, Polytechnique Montréal, 2500 chemin de Polytechnique, Montreal, Quebec, Canada
6Department of Clinical Neurosciences, University of Calgary, 3330 Hospital Drive N.W. HRIC 1B37A, Calgary, Alberta, T2N 4N1, Canada
 # J.R.G. and C.H.A. contributed equally to this work.
** Corresponding author: smurugkar@physics.carleton.ca*

This document provides Supplementary Information for "Spectral focusing-based stimulated Raman scattering microscopy using compact glass blocks for adjustable dispersion". In Section S1, we summarize a theoretical treatment to predict the pulse width of pulses chirped within glass blocks and compare these theoretical predictions to our experimentally determined pulse widths. In Section S2, we show how these results can be used to calculate the chirp ratio of the pulses, as well as predict the spectral resolution of our system for a given number of bounces within the variable-length glass blocks. In Section S3, we explain the procedure behind the calculation of spectral range of the system.

S1 - Theoretical determination of pulse width and comparison to experimental values

To obtain the temporal width of the pulses, an initial pulse with zero chirp is assumed to have a temporal width of τ_0 and wavelength λ. Each glass optic will then induce group delay dispersion (GDD) in the pulse, chirping it. The GDD can be obtained by multiplying the group velocity dispersion (GVD) of the TIH53 glass times the length of glass propagated L . The GVD for a given material is related to the second derivative of the material's index of refraction $n(\lambda)$ with respect to wavelength by

$$GVD = \frac{\lambda^3}{2\pi c^2}\frac{d^2n}{d\lambda^2}, \tag{1}$$

where c is the speed of light. An equation for n as a function of λ to calculate the GVD can be obtained by using the Sellmeier equation for $n(\lambda)$, which is given by

$$n(\lambda) = \sqrt{1 + \sum_i^m \frac{B_i \lambda^2}{\lambda^2 - C_i}}. \quad (2)$$

Here, λ is the wavelength (in microns), and the parameters B_i and C_i are empirically determined for a given glass. For TIH53 glass, these parameters are:

	1	2	3
B	1.879	0.3697	2.337
C	0.01441	0.06388	182.7

Table S1: Parameters B1–B3 and C1–C3 for TIH53 glass.

The second derivative of the refractive index with respect to wavelength is given by

$$\frac{d^2n}{d\lambda^2} = \frac{1}{n\lambda^4}\left(\sum_i^m \frac{B_i C_i}{(1 - C_i)^2}\left[3 + \frac{4C_i}{(1 - C_i)\lambda^2}\right]\right) - \frac{1}{n}\left(\frac{dn}{d\lambda}\right)^2, \quad (3)$$

$$\frac{dn}{d\lambda} = -\frac{1}{n\lambda^3}\left(\sum_i^m \frac{B_i C_i}{\left(1 - \frac{C_i}{\lambda^2}\right)^2}\right). \quad (4)$$

For the wavelengths used in the main paper, the GVD values are as follows:

GVD values		
796 nm	942 nm	1040 nm
221 000 fs^2/m	171 000 fs^2/m	145 000 fs^2/m

Table S2: GVD values of TIH53 glass at wavelengths of 796 nm, 942 nm, and 1040 nm.

In the main paper, the glass blocks are used with 2, 3, 4, 6, 7, and 8 bounces, corresponding to the following propagation distances within the glass blocks: 26 cm, 36 cm, 46 cm, 66 cm, 76 cm, and 86 cm. The bounce numbers used in the main paper correspond to the following GDD values:

Wavelength (nm)	GDD after propagating through TIH53 glass block (fs^2)					
	2 bounces	3 bounces	4 bounces	6 bounces	7 bounces	8 bounces
796	57 500	79 600	102 000	146 000	168 000	190 000
942	44 300	61 400	78 500	113 000	130 000	147 000
1040	37 800	52 400	66 900	96 000	111 000	125 000

Table S3: GDD values for different lengths of TIH53 glass at wavelengths of 796 nm, 942 nm, and 1040 nm.

With the calculated GDD values, the temporal width τ_p is calculated for a Gaussian pulse with the equation

$$\tau_p = \sqrt{1 + \left(\frac{4 \log 2 \, GDD}{\tau_0^2}\right)^2}\,\tau_0. \quad (5)$$

We obtain our value for the pre-chirp pulse width (τ_0) by measuring the output pulse of the laser with an autocorrelator. The following values were obtained for the pulses at 796 nm, 942 nm, and 1040 nm:

Pre-chirp pulse duration		
796 nm	942 nm	1040 nm
169 fs	157 fs	210 fs

Table S4: τ_0 values for pulses at 796 nm, 942 nm, and 1040 nm.

We may now calculate the theoretical values for the pulse widths predicted by this theoretical treatment. We calculate pulse widths for transform-limited pulses of wavelengths 796 nm, 942 nm, and 1040 nm propagating through a given amount of TIH53 glass defined by the number of bounces (see main text). These theoretical predictions, as well as the experimentally determined values, are shown below in Table S5.

Wavelength (nm)	Theoretical pulse width after propagating through TIH53 glass block					
	2 bounces	3 bounces	4 bounces	6 bounces	7 bounces	8 bounces
796	0.92 ps	1.28 ps	1.64 ps	2.36 ps	2.73 ps	3.09 ps
942	0.77 ps	1.07 ps	1.36 ps	1.96 ps	2.26 ps	2.57 ps
1040	0.52 ps	0.70 ps	0.89 ps	1.27 ps	1.46 ps	1.65 ps
Wavelength (nm)	Experimental pulse width after propagating through TIH53 glass block					
	2 bounces	3 bounces	4 bounces	6 bounces	7 bounces	8 bounces
796	0.78 ps	1.16 ps	1.47 ps	—	—	—
942	—	—	—	1.77 ps	2.10 ps	2.39 ps
1040	0.55 ps	0.65 ps	0.77 ps	0.94 ps	1.10 ps	1.26 ps

Table S5: Theoretical and experimentally determined pulse widths at 796 nm, 942 nm, and 1040 nm for different lengths of TIH53 glass.

The experimental values deviate from the theoretical values by the percentages provided in Table S6:

Wavelength (nm)	Experimental values versus theoretical values					
	2 bounces	3 bounces	4 bounces	6 bounces	7 bounces	8 bounces
796	18%	10%	12%	—	—	—
942	—	—	—	11%	8%	8%
1040	5%	8%	16%	35%	33%	31%

Table S6: Percentage difference between theoretical and experimental values in Table 5.

This difference between the experimentally measured and theoretical values is due to a discrepancy in the values of the pre-chirp pulse duration (Table S4) of the pump and Stokes beams. This is most likely due to both the uncertainty in the autocorrelator measurement used to estimate this value and due to the laser pulses directly out of the laser not being transform-limited owing to internal dispersion compensation.

S2 - Calculation of chirp ratio and spectral resolution as a function of pulse width

The relationship between the chirp ratio and the pulse width pre-chirp and post-chirp can be obtained by using Eq. (5) as well as the equation[1,2]

$$\beta = \frac{2GDD}{\tau_0^2 + 4GDD^2}. \tag{6}$$

Here, τ is the pulse width after chirping for a Gaussian pulse, τ_0 is the pulse width of the unchirped Gaussian transform-limited pulse, GDD is the group delay dispersion, and β is the chirp parameter of the pulse. Both equations may be combined to factor out the GDD, yielding an equation for the chirp parameter as a function of the pulse width pre- and post-chirp:

$$\beta = \frac{\sqrt{\tau^2/\tau_0^2 - 1}}{2\ln 2\,\tau_0^2\left(1 + \frac{1}{(2\ln 2)^2}(\tau^2/\tau_0^2 - 1)\right)}. \tag{7}$$

This equation can be used to calculate the chirp ratio β_p/β_s, where β_p is the chirp of the pump and β_s is the chirp of the Stokes after having traversed through the glass blocks. For an identical number of bounces in the pump and Stokes, the chirp ratios are provided below, for each relevant pump wavelength:

Chirp ratio			
CH region		Fingerprint region	
Number of bounces	796 nm	Number of bounces	942 nm
2–2	0.84	6–6	0.89
3–3	0.76	7–7	0.88
4–4	0.72	8–8	0.87

Table S7: Theoretical estimates of chirp ratio in the CH and fingerprint regions when using different numbers of bounces.

The spectral resolution can be obtained in terms of the pump and Stokes pulse widths τ_p and τ_s by using the following equation, which is valid for chirp-matched pulses[1,2]:

$$\Delta\nu = \frac{2\ln 2}{\pi c}\sqrt{2\left(\tau_p^{-2} + \tau_s^{-2}\right)}. \tag{8}$$

In the case of pulses that are not precisely chirp-matched, an additional chirp mismatch term is added which compensates for the lack of chirp matching:

$$\Delta\nu_{\Delta\beta} = \frac{|\Delta\beta|}{\pi c\sqrt{\tau_p^{-2} + \tau_s^{-2}}}. \tag{9}$$

These equations can then be used to predict the spectral resolution as a function of the theoretically predicted pulse durations. The τ_0 values of our system are provided in section S1. In combination with the pulse widths determined in the previous section, the total spectral

resolution when factoring in mismatch can be calculated. These values, with and without factoring the added resolution from mismatch, are provided below:

Spectral resolution (cm^{-1})					
CH region			Fingerprint region		
Number of bounces	Spectral resolution	Spec. res. with mismatch	Number of bounces	Spectral resolution	Spec. res. with mismatch
2–2	36.0	43.7	6–6	15.7	22.1
3–3	26.5	39.7	7–7	13.7	20.5
4–4	20.9	37.0	8–8	12.1	19.4

Table S8: Theoretical estimates of spectral resolution with and without mismatch in the CH and fingerprint regions when using different numbers of bounces.

The measured spectral resolution values are better than the theoretical predictions. This is likely due to the discrepancy in the measured pre-chirp, transform-limited values of the pump and Stokes pulses as mentioned above.

S3 - Calculation of spectral range

The spectral range of the system was calculated by using a sample of rhodamine 6G in methanol (50 μM). The rhodamine 6G spectrum is obtained by acquiring the two-photon absorption (2PA) intensity of the rhodamine sample as a function of the delay line position. The spectral range can then be obtained from the full-width at half-maximum of the 2PA spectrum (Fig. S1). The calibration of the delay line position to the wavenumber of the Raman shift was performed using the method outlined in the main text with a DMSO sample.

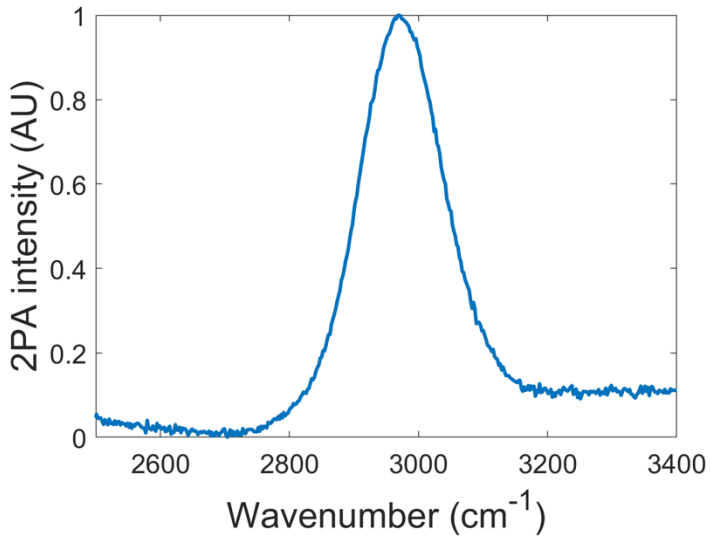

Fig. S1: Two-photon absorption intensity spectrum of Rhodamine 6G sample. The signal dips under the background level to the left of the spectrum due to saturation effects on the rhodamine sample by the Stokes pulse, which leads the pump pulse for smaller delay line positions.

1. M. Mohseni, C. Polzer, and T. Hellerer. Resolution of spectral focusing in coherent Raman imaging. *Opt Express* **26**, 10230 (2018).

2. R. A. Cole and A. D. Slepkov. Interplay of pulse bandwidth and spectral resolution in spectral-focusing CARS microscopy. *Journal of the Optical Society of America B* **35**, 842 (2018).